

1 Article

2 Allosteric effects between the Antibody constant and 3 variable regions: A study of IgA Fc mutations on 4 antigen binding

5 Chinh Tran-To Su^{1#}, Wai-Heng Lua^{1#}, Wei-Li Ling¹, and Samuel Ken-En Gan^{1,2,*}

6 ¹ Bioinformatics Institute, Agency for Science, Technology and Research (A*STAR), Singapore

7 ² p53 Laboratory, Agency for Science, Technology and Research (A*STAR), Singapore

8 * Correspondence: samuelg@bii.a-star.edu.sg; Tel.: +65-6478 8317

9 # Authors equally contribute to the work

10

11 **Abstract:** Therapeutics antibodies have increasingly shifted the paradigm of disease treatments,
12 from small molecules to biologics, especially in cancer therapy. Despite the increasing number of
13 antibody candidates, much remains unknown about the antibody and how its various regions
14 interact. In fact, the constant region can govern effects that might be useful in reducing the
15 unwanted consequences resulted from systemic circulation. For this reason, apart from the
16 commonly used IgG isotypes, IgA antibodies are promising therapeutics drugs, given its localized
17 mucosal effects. While the antibody Fc effector cell activity has been well explored, recent research
18 has shown evidences that the constant region of the antibody can also influence antigen binding,
19 challenging the conventional idea of region-specific antibody functions. To further investigate this,
20 we analyzed the IgA antibody constant and its allosteric effects onto the antigen binding regions,
21 using recombinant Pertuzumab IgA1 and IgA2 variants. We found mutations in the C-region to
22 reduce Her2 binding, and our computational structural analysis showed that such allosteric
23 communications were highly dependent on the antibody hinge, providing the evidence to consider
24 antibodies as a whole protein rather than a sum of functional regions.

25 **Keywords:** Antibody; Isotype IgA; Pertuzumab; Allosteric; biologics; constant region; variable
26 region
27

28 1. Introduction

29 Antibodies, also known as the “magic bullet” by Paul Ehrlich [1-3], have shown great promise
30 as therapeutic agents against numerous diseases [4] with many breakthroughs aimed at improving
31 its therapeutic effects [5-10]. One such promise is the use of IgA antibodies over the reigning IgG
32 isotypes in therapy [9-12], especially given the activation and localization of IgA, where
33 predominantly mucosal, may have reduced systemic circulations and the associated side effects.

34 IgA (IgA1 and IgA2) is the major immunoglobulin isotype in adaptive mucosal immunity
35 [13-16] that can lead to several disease pathologies such as IgA Nephropathy when they polymerize
36 or self-aggregate [17,18]. Recently, a chimeric IgG-A antibody (with engineered CH₂-CH₃ Fc
37 region [19]) showed greater killing of Her2 cancer cells by higher levels of complement-dependent
38 cytotoxicity and activations of both neutrophils and macrophages. Although the chimeric IgG-A
39 utilized only the CH₃ domain, this example clearly shows that the Fc of antibodies can be
40 engineered towards various effector effects.

41 Fc manipulations have also been used to improve antibody half-lives [20], as well as to make
42 bispecific antibodies [8], or create “sweeping” antibodies [21]. However, the overall effects of such

43 constant region modifications on other antibody functions such as antigen bindings are not well
44 established. In recent decades, there are increasing reports [22-27] of distant effects between the Fc
45 region and the antigen-binding regions, likely allosteric communications, with investigations
46 predominantly performed on IgG antibodies.

47 Similar to the case of IgG [23,27], our previous work [26] demonstrated that the heavy chain
48 constant regions can modulate antigen binding, most obvious for IgM and IgD, and to a smaller
49 extent, IgA and its subtypes. To further investigate these effects, we generated mutations in the IgA
50 constant regions and measured the antigen binding. And at the same time, we carried out
51 computational analyses of allosteric communications between the constant and variable regions of
52 these IgA antibodies.

53

54 2. Materials and Methods

55 *Production of Recombinant Pertuzumab IgA antibodies*

56 Wild-type recombinant Pertuzumab IgA1 and IgA2 were gene synthesized and expressed as
57 were previously described [26]. The mutations (C266Y/H317R for IgA1 and C253Y/H304R for IgA2):
58 a conserved Cysteine and the other, randomly picked as control, were incorporated into the IgA
59 constant regions by site directed mutagenesis (Agilent Technologies, Cat no. 200521). Produced IgA
60 antibodies were quantified by spectrophotometric means using the extinction coefficient values
61 determined from ProtParam [28]. Gel filtration figures were generated from Unicorn 6.0 software
62 (GE Healthcare) with lines thickened using the GIMP 2.9.4 software. Purified antibody variants were
63 analysed on reducing 10% SDS-PAGE gels and stained using Bio-Safe Coomassie stain (Bio-Rad, Cat
64 no. 1610786). Gel band sizes were determined using GelApp [29].

65 *Binding affinity studies*

66 Binding kinetics (using Blitz®, Fortebio) of the antibodies to Her2 were carried out by
67 pre-binding of HIS-tagged Her2 (Sino Biologicals Inc, Cat no. H10004-H08H) onto the Ni-NTA
68 (NTA) biosensors (Fortebio, Cat no. 18-5101) as previously described and performed [26,30] using 1×
69 kinetic buffer.

70 *Modeling full antibody structures of IgA1 and IgA2*

71 Atomistic models of the two antibody variants IgA1 and IgA2 were constructed using two
72 scattering-solved structures PDB: 2QTJ and PDB: 1R70 as templates for the Fc region, respectively.
73 PDB: 1S78 was used as the template for the Pertuzumab Fab region. The resulting α -based
74 backbones of the Fc regions were then used to construct the full-atom backbones and side chains
75 using PULCHRA [31] and SCWRL4 [32], respectively. A standard procedure of energy minimization
76 (5000 steps using steepest descent followed by conjugate gradient) was performed to remove
77 possible clashes, using AMBER 14 [33]. Mutant IgA1 and IgA2 structures were modelled with
78 corresponding mutations C266Y/H317R and C253Y/H304R, respectively.

79 The energy-minimized structures of the two variants (each including the wild type and mutant)
80 were then subjected to coarse grain simulation (using Martini force field for proteins combined with
81 *ElNeDyn* elastic network) to sample conformational changes of the whole antibody structures. The
82 simulations were performed with time steps (dt) gradually increased from 15 fs to 22 fs during the
83 equilibrium to accommodate ion wild motions, then fixed at $dt = 22fs$ during the production stages
84 ($3 \times 1 \mu s$) with Verlet algorithm. Periodic boundary condition was also applied to avoid the finite size
85 effects while simulating in explicit solvent (polarized water model; hence with PME). Temperature
86 and pressure coupling schemes were used with the velocity rescale (*V-rescale*) and the

87 Parrinello-Rahman barostat. Our analyses used the data from the last 600ns (x3) of the simulated
88 trajectories that reflected stable simulations, resulting in 3x1000 conformations.

89 *Quantification of allosteric effects*

90 We first used the minimized structures of the wild type variants IgA1 and IgA2 to quantify the
91 allosteric effects in both the Her2-binding and mutation events (as shown in Figure 1) using the
92 server AlloSigMA [34], which have demonstrated successful quantification of allosteric effects in
93 various benchmarked allosteric proteins [35-38]. The allosteric communications were estimated
94 based on the responses of each residue (via residual free energy change $\Delta g_{\text{residue}}$) with respect to
95 perturbations due to each of the events [34]. In this analysis, we simulated the mutations by
96 initiating perturbations at the substituted positions (i.e. assigning “Up-mutation” in the AlloSigMA
97 server to simulate larger residue substitutions). The resulting residue-wise allosteric free energies
98 (with negative values indicating stabilizing and positive values indicating destabilizing effects)
99 showed the quantified allosteric effect caused by the mutations. We then estimated the free energy
100 change at the Her2 binding site ($\Delta g_{\text{Her2site}}$) and other corresponding regions (Δg_{region}) by averaging all
101 $\Delta g_{\text{residue}}$ values of the involving residues.

102 In addition, we estimated and clustered the distance ratio (i.e. distances between center-of-mass
103 of Fab regions versus those of both Fab and Fc as shown in Figure 2) of the wild type structures
104 resulting from the coarse grain simulation. Conformations nearest to the centroids were extracted
105 and reverted to atomistic structures using Charmm36 force field and TIP3P water model, followed
106 by short minimization and equilibrium. The structures were then used to study the spectrum of the
107 allosteric effect driven by the domain motions (as shown in Table 3).

108

109 **Data Availability**

110 The datasets generated and/or analyzed during the current study are available upon reasonable
111 request.

112

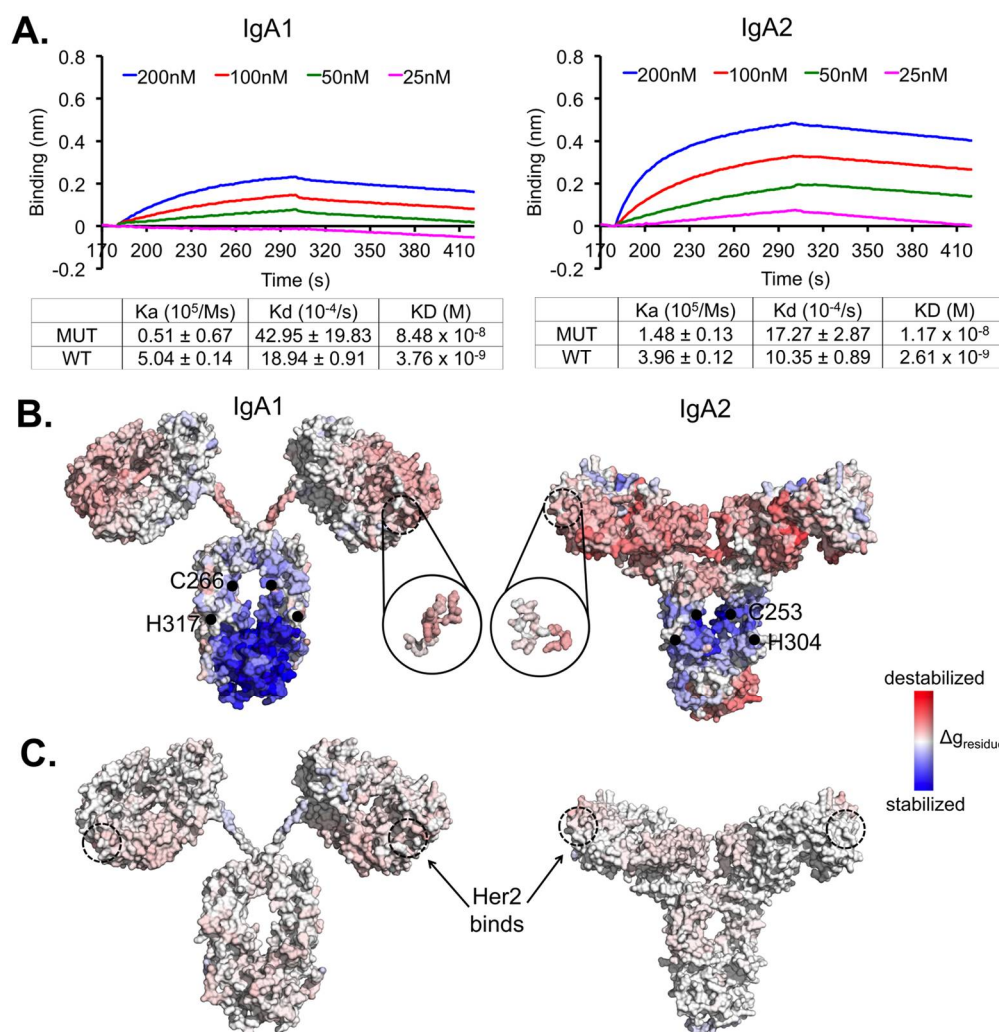
113

114 **3. Results**

115 Our previous work [26] suggested that the heavy chain constant regions, but not light chain
 116 constant regions, influence antigen binding beyond simple avidity effects, e.g. IgM. To further
 117 investigate this phenomenon, we generated several disruptive mutations: C266Y/H317R in IgA1 and
 118 C253Y/H304R in IgA2 at the heavy chain constant region (CH α 3) of our Pertuzumab IgA1 and IgA2
 119 (i.e. substituting one of the disulfide-forming Cysteine residues in the CH3 domain with the bulky
 120 residue Tyrosine and another randomly selected Histidine residue with similar positively charged
 121 Arginine) to deliberately affect the heavy chain stability, and subsequently detected corresponding
 122 effects on the Her2-binding region.

123 Experimentally, we found the recombinant transient expression of both mutant variants to drop
 124 drastically (multiple folds) compared to the wild types (data not shown). A higher rate of
 125 aggregation in the isotype mutants was also observed (Supplementary S1). In addition, our binding
 126 kinetics measurements showed a significant decrease of the mutants by a log at 10^{-8} compared to the
 127 wild type at 10^{-9} for both IgA1 and IgA2. The major effects on IgA1 as we have found, were at the
 128 association constant measurements for IgA1 and to a reduced extent, at the dissociation constant,
 129 whereas for IgA2, the differences were less pronounced on both the association and dissociation
 130 constants. (Figure 1A).

131



132

133 **Figure 1.** Synergistic allosteric effects by the two IgA1 and IgA2 constant region mutations on the
 134 Her2-binding variable regions. **(A)** Binding kinetics analysis of the isotype variants IgA1 and IgA2 to
 135 Her2, using the antibodies at 200nM to 25nM to pre-loaded Her2 on NTA biosensors. The binding
 136 kinetics was measured using Blitz®. All experiments were performed in triplicates independently.
 137 The binding kinetics values of the wild type IgA1 and IgA2 shown were obtained from our previous

138 work [26]. (B) Surface presentations of the quantified allosteric communications (presented by
 139 residual allosteric free energy change $\Delta g_{\text{residue}}$) demonstrate destabilizing effects on the Her2 binding
 140 region caused by the mutations (black dots) in both the mutant constant region variants. (C) The
 141 quantified allosteric effects shown were based on the event of Her2 bindings. In both (B) and (C), the
 142 effects were estimated using the minimized structures of both the wild type IgA subtypes for
 143 perturbations with respect to mutating or binding events.

144 Our experimental observations show that mutation-driven perturbations in the constant
 145 regions can affect Her2 binding, even with few substitution mutations, indicating clear allosteric
 146 communications between the two regions. We applied a structure-based statistical mechanical
 147 model [38] (implemented in the AlloSigMA server [34]) to quantify these underlying allosteric
 148 effects. Results showed that the mutations caused stabilizing effects in the Fc region (Figure 1B and
 149 Table 1). This stabilization was compensated by increasing energy gain in distant regions, in this
 150 case the V-regions, thus resulting in destabilizing effects onto the Her2 binding site, i.e. causing it to
 151 be more flexible (with $\Delta g_{\text{Her2site}} > 0$) due to contact losses between the Her2-interacting residues and
 152 their neighbors (Table 2). Particularly, this destabilizing effect is more pronounced in the IgA1
 153 mutant (Table 3 and Supplementary S2).

154
 155 **Table 1.** Accumulative allosteric effect on various regions (represented by Δg_{region}) using the
 156 minimized structures of IgA1 and IgA2, when mutated or when bound to Her2.
 157

Region	Δg_{region} (kcal/mol)			
	Mutating event		Her2-binding event	
	IgA1	IgA2	IgA1	IgA2
Her2 binding site	0.18	0.12	0.06	-0.05
Fab	0.15	0.38	0.08	0.02
Fc (CH2-CH3)	-0.46	-0.08	0.03	-0.007
Hinge	0.05	0.04	-0.02	0.03

158 We independently initiated computational perturbations at the Her2-binding site and studied
 159 the Fc responses in both the variants to simulate the back-and-forth signal propagations between the
 160 two regions (Figure 1B and 1C). When comparing between the two events of mutations and
 161 Her2-binding, we noticed energy compensation to occur at the Fab regions of both IgA1 and IgA2.
 162 The IgA2-Fab domain compensated significantly more than that of IgA1 on the whole, distributing
 163 the energy compensation across the entire region, thus balancing the destabilization at the Her2
 164 binding site (as $\Delta g_{\text{Her2site}}^{\text{IgA2}} < \Delta g_{\text{Her2site}}^{\text{IgA1}}$) and retaining more of the binding ability to Her2. On the
 165 other hand, the energy compensation in the IgA1 Fab is likely to have partially accommodated for
 166 the changes at the hinge in terms of rigidity when the allosteric signal was transferred via its long
 167 Proline-rich hinge (Figure 1B). This might not be the case for the IgA2 short hinge, suggesting that
 168 the allosteric communication barrier was lifted when the hinge became more flexible (Table 1 and 3).
 169
 170

171 **Table 2.** Percentages* of native contacts (%) in the minimized structures of IgA1 and IgA2
 172 mutants, showing the contact loss as compared to the wild type.
 173

	All heavy atoms / C α atoms	
	IgA1	IgA2
Wild type	100 / 100	100 / 100
Mutant (replicate 1)	69.7 / 58.3	57.1 / 61.8
Mutant (replicate 2)	66.5 / 56.7	55.7 / 61.8
Mutant (replicate 3)	66.5 / 56.7	54.7 / 61.8

174 *Percentage = (number of native contacts in mutant) / (number of native contacts in wild type)
 175

176 Meanwhile, we hypothesized that the two mutation positions have functional selection
 177 constraints. To test this, we used the EVcoupling server [39] to investigate the residue couplings of
 178 the constant and variable regions (results of which demonstrate the local proximity as well as
 179 contacts in the antibody variants under the function dependent constraints). We found strong
 180 residue coupling networks forming independently within domains Fab or Fc, but weak links
 181 between the two domains (Figure 2). Particularly in the Fc domain, only the Cysteine residue (C266
 182 in IgA1 or C253 in IgA2) exhibited moderate functional dependence, as expected for a conserved
 183 Cysteine.

184 When additionally performing single perturbations at the individual positions, we found the
 185 allosteric signals to be contributed significantly by the substitution of the Histidine (H317 in IgA1 or
 186 H304 in IgA2) with a larger residue. Interestingly, the highly conserved disulfide-forming Cysteine
 187 contributed less effect to destabilizing the Her2 binding site (Table 3). These results indicate that the
 188 two domains Fab and Fc clearly communicate with each other and that the Histidine position might
 189 play a bigger role in the communications. In addition, we found the destabilizing effect on the
 190 Her2-binding site to be a result of accumulative signaling, particularly facilitated via the hinge.
 191 Therefore, the effect caused by the Fc mutations on the Her2 binding ability of the Fab domain
 192 (Figure 1A) is modulated by the flexibility of the hinge.

193 The IgA1 isotype contains a longer hinge (connecting CH1 and the rest of the Fc region), the
 194 flexibility of which amplified with the mutation events (with $\Delta g_{hinge}^{IgA1} = 0.21 \pm 0.20$ whereas Δg_{hinge}^{IgA2}
 195 $= 0.08 \pm 0.05$). Scattering experiments on the wild type IgA1 isotype (PDB: 2QTJ) showed that rigid
 196 flanking hinge, which distances the two regions Fab and Fc in an extended IgA1 conformation in
 197 solution, is favored. Our dynamics simulations of the wild type IgA1 structure also showed that the
 198 two regions remained relatively constant proximity to each other. However, more diverse domain
 199 fluctuations between the two regions were observed in the conformational sampling of the IgA1
 200 mutant (Figure 2A, top right), implying a structural interference caused by the mutations to the
 201 hinge flexibility. On the other hand, the shorter IgA2 hinge did not allow for wild domain motions
 202 (Figure 2B, top right). While the Her2-binding ability is mostly abolished in the IgA1 mutant, it is
 203 retained in the IgA2 mutant, suggesting that hinge flexibility modulates the propagation of the
 204 allosteric signals between the two distant domains.

205

206 **Table 3.** Allosteric free energy (Δg_{region}) estimated in mutation events (accumulative or single
 207 mutations) using different conformations of the wild type variants IgA1 and IgA2

208

	Δg_{region} (kcal/mol) in the event of mutations					
	IgA1 (C266/H317)	IgA2 (C253/H304)	IgA1 (C266)	IgA2 (C253)	IgA1 (H317)	IgA2 (H304)
Her2 site	0.38 ± 0.32	0.12 ± 0.06	0.18 ± 0.16	0.06 ± 0.07	0.28 ± 0.23	0.09 ± 0.05
Fab	0.62 ± 0.54	0.31 ± 0.12	0.28 ± 0.26	0.23 ± 0.09	0.5 ± 0.36	0.13 ± 0.08
Fc (CH2-CH3)	-0.52 ± 0.05	-0.16 ± 0.27	-0.4 ± 0.07	-0.06 ± 0.29	-0.25 ± 0.09	-0.1 ± 0.03
Hinge	0.21 ± 0.2	0.08 ± 0.05	0.08 ± 0.09	-0.003 ± 0.032	0.20 ± 0.17	0.07 ± 0.04

209

210

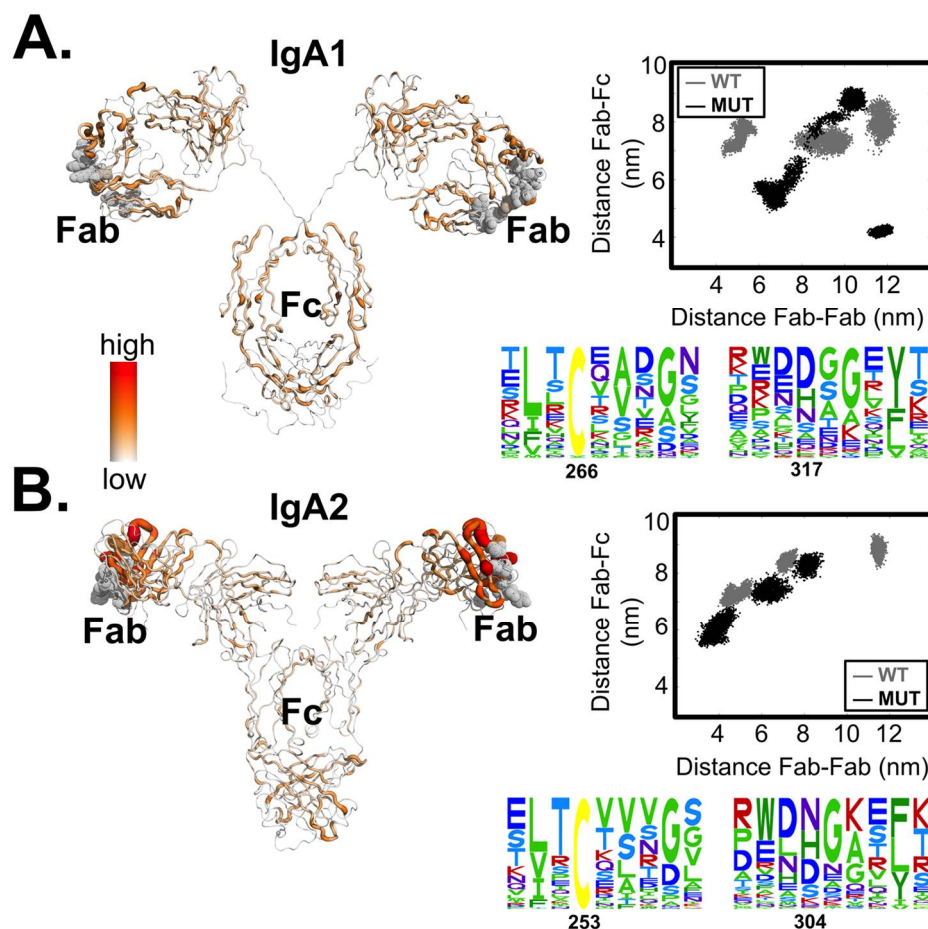


Figure 2. Residue couplings and hinge-dependent domain proximity of the two variants IgA1 (in A) and IgA2 (in B). The sequence alignments of the mutation regions were performed using the EVcoupling server [39] and the coupling values were mapped back to the minimized structures of the variants. Distances were estimated between the center of mass of the Fc region and that of the Her2-binding sites. Note that in the distance distributions of the IgA2 mutant (in B) showed the plotted values obtained from two replicates that successfully reached equilibrium in the given time scales.

211
212
213
214
215
216
217
218

219 4. Discussion

220 We set out to investigate the mechanism of the allosteric effects that the antibody constant
221 regions elicited on the antigen binding as suggested in our previous work [26]. Working on our IgA1
222 and IgA2 models, we sought to study such effects in greater details by analyzing the effects of Her2
223 binding when two mutations were introduced, at a conserved Cysteine (C266/C253) and a random
224 selected control Histidine (H317/H304). While we acknowledge that the starting structure
225 dependency remains a challenge in our approach (e.g. input into the AlloSigMA server [34] to
226 account for the entropic contribution in the allosteric free energy changes), we have general
227 agreement between the computational and experimental results, where the computational
228 observations could provide us an insight to the allostery phenomenon between the variable and
229 constant regions.

230 Experimentally, we found that the double mutants were produced at a significantly reduced
231 rate in our transient expressions, and that there were compromises in terms of binding ability to
232 Her2, albeit at different magnitudes, despite intact and unchanged variable regions. This further
233 demonstrated that the constant region had significant major effects on antigen binding, agreeing
234 with other such studies on IgGs [22,23,25], although this is in the IgA context. To understand the
235 mechanism underlying our experimental observations, we showed that the allosteric signaling
236 propagated back-and-forth between the two distant regions, from Her2-binding region to the Fc

237 region and vice versa, on the IgA isotypes. In fact, the domain-linking hinge mediated such
238 communication signaling, demonstrating that the allosteric effects were moderated by the hinge
239 flexibility, particularly at the level of energy compensations at the distal regions.

240 We postulated that the energy compensation at the Fabs of the IgAs variants to accommodate
241 the flexibility changes upon balance at the Her2-binding site (Table 1 and 3) to maintain the
242 Her2-binding ability. As a result, our findings partially agree with several previous studies [40-42]
243 that the antigen-binding region requires a certain level of rigidity. On the contrary, other studies
244 [43,44] suggested no significant conformational differences found in these regions, perhaps due to
245 the different antigens. It should also be noted that many of these previous studies were performed
246 on antibody fragments, e.g. Fab or Fv, and not on IgA. Thus, together with our other findings
247 [26,27,45,46] also involving other proteins, we have shown the need to examine proteins as a whole
248 for more comprehensive holistic investigations, especially on allostery. In particular to the context of
249 whole antibody, we found the hinge rigidity and the allosteric communications between the distant
250 constant and variable regions both to contribute to antigen binding.

251 Our results here are also consistent with other previous studies [22,24] that showed induced
252 conformational changes at the Fc due to the binding of antigen, hence consequently regulating the Fc
253 receptor binding. We thus believe there should exist a network of allosteric residues that drive the
254 allosteric signaling between the regions. Our future work hence will explore hotspots or mutation
255 boundaries that can improve antigen binding by taking the advantages of allosteric communications
256 from constant regions towards a rational and targeted approach for Fc engineering.

257 In conclusion, using both an experimental and computational approach, we were able to show
258 that the constant region is important in the ability of the variable regions in binding antigens. We
259 showed this is the less studied IgA, and that such effects were computationally found to be mediated
260 by the hinge region of the antibody. This further illustrates the need to consider antibodies as a
261 whole, rather than merely a sum of its regions.

262
263

264 **Supplementary Materials:** The following are available online at www.mdpi.com/link, Figure S1: Pertuzumab
265 isotype/subtype biophysical analysis.

266

267 **Acknowledgments:** This work was supported by the Agency for Science, Technology, and Research (A*STAR)
268 Joint Council Office (JCO1334i00050) and the A*STAR BioMedical Research Council Young Investigator Grant
269 (BMRC YIG 1510651021) in Singapore. We thank Santhosh Kumar Karthikeyan, Phua Ser Xian, Jonathan
270 Kuan-Wai Tham, Chua Hua Lun, Ryan Chang, Joshua Yi Yeo, and Chan Kwok Fong for their helps in
271 generating AlloSigMA data.

272

273 This paper is submitted along with a submission invitation by Dr Buyong Ma from National Cancer Institute,
274 NIH, Frederick.

275

276 **Author Contributions:** CTTS designed and performed the computational analyses. WHL and WLL performed
277 wet-lab experiments. WHL, CTTS, and SKEG analyzed the results. CTTS, WHL, and SKEG wrote the
278 manuscript. SKEG supervised the whole study. All authors read and approved the manuscript.

279

280 **Conflicts of Interest:** The authors declare no conflict of interest.

281 References

- 282 1. Strebhardt, K.; Ullrich, A. Paul Ehrlich's magic bullet concept: 100 years of progress. *Nature*
283 *Reviews Cancer* **2008**, *8*, 473-480.

- 284 2. Kohler, G.; Milstein, C. Continuous cultures of fused cells secreting antibody of predefined
285 specificity. *Nature* **1975**, 495-497.
- 286 3. Ehrlich, P. Über den jetzigen Stand der Karzinomforschung. *Beiträge zur experimentellen*
287 *Pathologie und Chemotherapie* **1909**, 117-164 (in German).
- 288 4. Strohl, W.R. Current progress in innovative engineered antibodies. *Protein Cell* **2018**, 9,
289 86-120.
- 290 5. Igawa, T.; Ishii, S.; Tachibana, T.; Maeda, A.; Higuchi, Y.; Shimaoka, S.; Moriyama, C.;
291 Watanabe, T.; Takubo, R.; Doi, Y., *et al.* Antibody recycling by engineered pH-dependent
292 antigen binding improves the duration of antigen neutralization. *Nat Biotechnol* **2010**, 28,
293 1203-1207.
- 294 6. Robinson, M.; Ke, N.; Lobstein, J.; Peterson, C.; Szkodny, A.; Mansell, T.; Tuckey, C.; Riggs,
295 P.; Colussi, P.; Noren, C., *et al.* Efficient expression of full-length antibodies in the cytoplasm
296 of engineered bacteria. **2015**.
- 297 7. Park, H.; Yoon, H.; Jung, S. The highly evolvable Antibody Fc domain. *Trends Biotechnol.*
298 **2016**, 34, 895-908.
- 299 8. Ha, J.; Kim, J.; Kim, Y. Immunoglobulin Fc heterodimer platform technology: From design to
300 applications in therapeutic antibodies and proteins. *Front Immunol* **2016**, 7, 394.
- 301 9. Leusen, J. IgA as therapeutic antibody. *Mol. Immunol.* **2015**, 68, 35-39.
- 302 10. Valerius, T.; Stockmeyer, B.; van Spriël, A.; Graziano, R.; van den Herik-Oudijk, I.; Repp, R.;
303 Deo, Y.; Lund, J.; Kalden, J.; Gramatzki, M., *et al.* FcαRI (CD89) as a novel trigger molecule
304 for bispecific antibody therapy. *Blood* **1997**, 90, 4485-4492.
- 305 11. Bakema, J.E.; Egmond, M.v. Immunoglobulin A. *mAbs* **2011**, 3, 352-361.
- 306 12. Leusen, J.H. IgA as therapeutic antibody. *Molecular Immunology* **2015**, 68, 35-39.
- 307 13. Schroeder, H.J.; Cavacini, L. Structure and function of immunoglobulins. *J Allergy Clin*
308 *Immunol* **2010**, 125, S41-52.
- 309 14. Woof, J.M.; Kerr, M.A. IgA function – variations on a theme. *Immunology* **2004**, 113, 175-177.
- 310 15. Chen, K.; Cerutti, A. The function and regulation of Immunoglobulin D. *Curr Opin Immunol.*
311 **2011**, 23, 345-352.
- 312 16. Preud'homme, J.-L.; Petit, I.; Barra, A.; Morel, F.; Lecron, J.-C.; Lelievre, E. Structural and
313 functional properties of membrane and secreted IgD. *Mol. Immunol.* **2000**, 37, 871-887.
- 314 17. Bonner, A.; Perrier, C.; Corthesy, B.; Perkins, S.J. Solution structure of human secretory
315 component and implications for biological function. *Journal of Biological Chemistry* **2007**, 282,
316 16969-16980.
- 317 18. Bonner, A.; Furtado, P.; Almogren, A.; Kerr, M.; Perkins, S. Implications of the near-planar
318 solution structure of human myeloma dimeric IgA1 for mucosal immunity and IgA
319 nephropathy. *J Immunol.* **2008**, 180, 1008-1018.
- 320 19. Kelton, W.; Mehta, N.; Charab, W.; Lee, J.; Lee, C.-h.; Kojima, T.; Kang, T.H.; Georgiou, G.
321 IgGA: a "Cross-Isotype" engineered human Fc antibody domain that displays both IgG-like
322 and IgA-like effector functions. *Chemistry & Biology* **2014**, 21, 1603-1609.
- 323 20. Borrok, M.; Mody, N.; Lu, X.; Kuhn, M.; Wu, H.; Dall'Acqua, W.; Tsui, P. An "Fc-Silenced"
324 IgG1 format with extended half-life designed for improved stability. *J Pharm Sci.* **2017**, 106,
325 1008-1017.

- 326 21. Igawa, T.; Maeda, A.; Haraya, K.; Tachibana, T.; Iwayanagi, Y.; Mimoto, F.; Higuchi, Y.; Ishii,
327 S.; Tamba, S.; Hironiwa, N., *et al.* Engineered monoclonal antibody with novel
328 antigen-sweeping activity in vivo. *PLoS ONE* **2013**, *8*, e63236.
- 329 22. Zhao, J.; Nussinov, R.; Ma, B. Antigen induced dynamic conformation changes of antibody
330 to facilitate recognition of Fc receptors. *Biophys J* **2018**, *114*, Supplement 1, p233a.
- 331 23. Janda, A.; Bowen, A.; Greenspan, N.S.; Casadevall, A. Ig constant region effects on Variable
332 region structure and function. *Front Microbiol* **2016**, *7*.
- 333 24. Oda, M.; Kozono, H.; Morii, H.; Azuma, T. Evidence of allosteric conformational changes in
334 the antibody constant region upon antigen binding. *Int Immunol.* **2003**, *15*, 417-426.
- 335 25. Yang, D.; Kroe-Barrett, R.; Singh, S.; Roberts, C.J.; Laue, T.M. IgG cooperativity – Is there
336 allostery? Implications for antibody functions and therapeutic antibody development. *mAbs*
337 **2017**, *9*, 1231-1252.
- 338 26. Lua, W.; Ling, W.; Yeo, J.; Poh, J.; Lane, D.; Gan, S. The effects of antibody engineering CH
339 and CL in Trastuzumab and Pertuzumab recombinant models: Impact on antibody
340 production and antigen-binding. *Sci Rep* **2018**, *8*, 718.
- 341 27. Ling, W.-L.; Lua, W.-H.; Poh, J.-J.; Yeo, J.Y.; Lane, D.P.; Gan, S.K.-E. Effect of VH-VL families
342 in Pertuzumab and Trastuzumab recombinant production, Her2 and Fc γ IIA binding. *Front*
343 *Immunol* **2018**, *9*.
- 344 28. Gasteiger, E.; Hoogland, C.; Gattiker, A.; Duvaud, S.; Wilkins, M.; Appel, R.; Bairoch, A.
345 Protein identification and analysis tools on the ExPASy server. In *The Proteomics Protocols*
346 *Handbook*, Walker, J.M., Ed. Humana Press: 2005; pp 571-607.
- 347 29. Sim, J.Z.; Nguyen, P.V.; Lee, H.K.; Gan, S. GelApp: mobile gel electrophoresis analyser. *Nat.*
348 *Methods Application Notes* **2015**.
- 349 30. Lua, W.H.; Gan, S.; Lane, D.; Verma, C. A search for synergy in the binding kinetics of
350 Trastuzumab and Pertuzumab whole and F(ab) to Her2. *NPJ Breast Cancer* **2015**, *11*.
- 351 31. Rotkiewicz, P.; Skolnick, J. Fast procedure for reconstruction of full-atom protein models
352 from reduced representations. *J Comput Chem* **2008**, *29*, 1460-1465.
- 353 32. Krivov, G.; Shapovalov, M.; Dunbrack, R.J. Improved prediction of protein side-chain
354 conformations with SCWRL4. *Proteins* **2009**, *77*, 778-795.
- 355 33. Case, D.A.; Berryman, J.T.; Betz, R.M.; Cerutti, D.S.; T.E. Cheatham, I.; Darden, T.A.; Duke,
356 R.E.; Giese, T.J.; Gohlke, H.; Goetz, A.W., *et al.* *AMBER 14*, University of California, San
357 Francisco, 2015.
- 358 34. Guarnera, E.; Tan, Z.W.; Zheng, Z.; Berezovsky, I.N. AlloSigMA: Allosteric Signalling and
359 Mutation Analysis server. *Bioinformatics* **2017**, *btx430*.
- 360 35. Chiang, R.; Gan, S.; Su, C. A computational study for rational HIV-1 non-nucleoside Reverse
361 Transcriptase inhibitor selection and discovery of novel allosteric pockets for inhibitor
362 design. *Bioscience Reports* **2018**.
- 363 36. Su, C.T.T.; Kwoh, C.K.; Verma, C.S.; Gan, S.K.E. Modeling the full length HIV-1 Gag
364 polyprotein reveals the role of its p6 subunit in viral maturation and the effect of
365 non-cleavage site mutations in protease drug resistance. *Journal of Biomolecular Structure and*
366 *Dynamics* **2017**.

- 367 37. Kurochkin, I.V.; Guarnera, E.; Wong, J.H.; Eisenhaber, F.; Berezovsky, I.N. Toward
368 allosterically increased catalytic activity of insulin-degrading enzyme against amyloid
369 peptides. *Biochemistry* **2017**, *56*, 228-239.
- 370 38. Guarnera, E.; Berezovsky, I.N. Structure-based statistical mechanical model accounts for the
371 causality and energetics of allosteric communication. *PLoS Comput Biol* **2016**, *12*, e1004678.
- 372 39. Hopf, T.A.; Colwell, L.J.; Sheridan, R.; Rost, B.; Sander, C.; Marks, D.S. Three-dimensional
373 structures of membrane proteins from genomic sequencing. *Cell* **2012**, *149*, 1607-1621.
- 374 40. Zimmermann, J.; Oakman, E.L.; Thorpe, I.F.; Shi, X.; Abbyad, P.; III, C.L.B.; Boxer, S.G.;
375 Romesberg, F.E. Antibody evolution constrains conformational heterogeneity by tailoring
376 protein dynamics. *Proc. Natl. Acad. Sci. USA* **2006**, *103*, 13722-13727.
- 377 41. Chong, L.T.; Duan, Y.; Wang, L.; Massova, I.; Kollman, P.A. Molecular dynamics and
378 free-energy calculations applied to affinity maturation in antibody 48G7. *Proc. Natl. Acad.*
379 *Sci. USA* **1999**, *96*, 14330-14335.
- 380 42. Li, T.; Tracka, M.B.; Uddin, S.; Casas-Finet, J.; Jacobs, D.J.; Livesay, D.R. Rigidity emerges
381 during Antibody evolution in three distinct antibody systems: Evidence from QSFR analysis
382 of Fab fragments. *PLoS Comput Biol* **2015**, *11*, e1004327.
- 383 43. Midelfort, K.; Hernandez, H.; Lippow, S.; Tidor, B.; Drennan, C.; Wittrup, K. Substantial
384 energetic improvement with minimal structural perturbation in a high affinity mutant
385 antibody. *J Mol Biol* **2004**, *343*, 685-701.
- 386 44. Jeliaskov, J.R.; Sljoka, A.; Kuroda, D.; Tsuchimura, N.; Katoh, N.; Tsumoto, K.; Gray, J.J.
387 Repertoire analysis of Antibody CDR-H3 loops suggests affinity maturation does not
388 typically result in rigidification. *Front Immunol* **2018**, *9*, 413.
- 389 45. Su, C.T.-T.; Ling, W.-L.; Lua, W.-H.; Poh, J.-J.; Gan, S.K.-E. The role of antibody V κ
390 Framework 3 region towards antigen binding: Effects on recombinant production and
391 Protein L binding. *Sci Rep* **2017**, *7*, 3766.
- 392 46. Phua, S.-X.; Lua, W.-H.; Gan, S.K.-E. Role of Fc α R EC2 region in extracellular membrane
393 localization. *Cell Cycle* **2018**.
- 394